ACS APPLIED MATERIALS & INTERFACES

Research Article

Cite This: ACS Appl. Mater. Interfaces 2020, 12, 238−249

www.acsami.org

Stimuli-Responsive Pure Protein Organogel Sensors and Biocatalytic Materials

Natasha L. Smith,[†] Andrew E. Coukouma,[†] David C. Wilson,[‡] Brenda Ho,[†] Vincent Gray,[†,§] and Sanford A. Asher*[,†]

[†]Department of Chemistry, University of Pittsburgh, Pittsburgh, Pennsylvania 15260, United States

[‡]FLIR Systems Inc., Pittsburgh, Pennsylvania 15238, United States

Supporting Information

ABSTRACT: Utilizing protein chemistry in organic solvents has important biotechnology applications. Typically, organic solvents negatively impact protein structure and function. Immobilizing proteins via cross-links to a support matrix or to other proteins is a common strategy to preserve the native protein function. Recently, we developed methods to fabricate macroscopic responsive pure protein hydrogels by lightly cross-linking the proteins with glutaraldehyde for chemical sensing and enzymatic catalysis applications. The water in the resulting protein hydrogel can be exchanged for organic solvents. The resulting organogel contains pure organic solvents as their mobile phases. The organogel proteins retain much of their native protein function, i.e., protein−ligand binding and enzymatic activity. A stepwise ethylene glycol (EG) solvent exchange was performed to transform these hydrogels into organogels with a very low vapor pressure mobile phase. These responsive organogels are not limited by solvent/mobile phase evaporation. The solvent exchange to pure EG is accompanied by a volume phase transition (VPT) that decreases the organogel volume compared to that of the hydrogel. Our organogel sensor systems utilize shifts in the particle spacing of an attached two-dimensional photonic crystal (2DPC) to report on the volume changes induced by protein−ligand binding. Our 2DPC bovine serum albumin (BSA) organogels exhibit VPT that swell the organogels in response to the BSA binding of charged ligands like ibuprofen and fatty acids. To our knowledge, this is the first report of a pure protein organogel VPT induced by protein−ligand binding. Catalytic protein organogels were also fabricated that utilize the enzyme organophosphorus hydrolase (OPH) to hydrolyze toxic organophosphate (OP) nerve agents. Our OPH organogels retain significant enzymatic activity. The OPH organogel rate of OP hydrolysis is ∼160 times higher than that of un-cross-linked OPH monomers in a 1:1 ethylene glycol/water mixture.

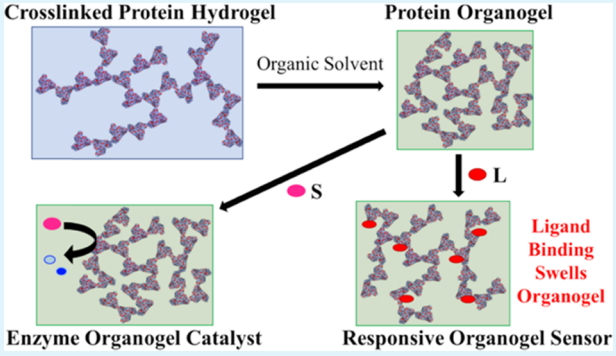

KEYWORDS: *responsive materials, protein organogels, protein hydrogels, protein immobilization, polymer volume phase transitions, nonaqueous enzymology, photonic crystal sensors, organophosphate decontamination*

INTRODUCTION

Hydrogels and organogels consist of three-dimensional polymer networks that utilize water or organic solvents as their mobile phases. Smart hydrogels and organogels contain functional groups such that the materials are responsive to chemical or physical stimuli such as pH,[1] light,[2] temperature,[3] or to chemical species.[4−6] These responsive materials have been designed for selective chemical sensing,[7] catalysis,[8] and drug delivery systems.[9]

Chemoselective responsive hydrogels[6] and organogels[10,11] often incorporate molecular recognition groups within the polymer networks. The molecular recognition event actuates selective chemical responses such as volume changes,[12] fluorescence,[13] or that trigger catalysis.[8,14] We developed multiple hydrogel chemical sensors by attaching molecular recognition groups that induce hydrogel volume phase transitions (VPTs) upon analyte binding.[6,15] This VPT response is understood in the context of the Flory polymer theory.[16−18] Chemical binding processes that induce Gibbs free-energy changes in the system generate osmotic pressures that swell or shrink the hydrogel or organogel. Small perturbations in the chemical environment can lead to remarkably large VPT.[18] Ultralow limits of analyte detection have been achieved by utilizing molecular recognition groups with large analyte binding affinities.[4]

Proteins serve many roles in biology, including molecular recognition. Proteins evolved highly efficient molecular recognition processes such as having large binding affinities for specific analytes and for carrying out highly selective enzymatic reactions. Highly chemoselective responsive hydro-

Received: October 7, 2019
Accepted: December 10, 2019
Published: December 10, 2019

DOI: 10.1021/acsami.9b18191
ACS Appl. Mater. Interfaces 2020, 12, 238−249

gels have been fabricated that utilize this protein molecular recognition.[4,14,19] For example, we fabricated organophosphate sensors with detection limits of ~4 fM by utilizing the extremely large binding affinity of organophosphates to acetylcholinesterase that was attached to polyacrylamide hydrogels.[4]

More recently, pure protein hydrogels were developed that consist of physically[8,9,20] or chemically[21−23] cross-linked proteins. Each protein monomer acts as a molecular recognition group to maximize the density of hydrogel functional groups. We designed several chemically cross-linked protein hydrogels for chemoselective two-dimensional photonic crystal (2DPC) sensor applications using human and bovine serum albumin (HSA and BSA),[5] concanavalin A (ConA),[24] and glucose binding protein.[25] These protein hydrogels retain similar ligand affinities as the native protein monomers. Protein−ligand binding that changes the Gibbs free energy actuates the VPT, which shifts the particle spacing of an embedded 2DPC. Particle spacing changes shift the 2DPC light diffraction and report on the hydrogel volume changes.[26] These pure protein hydrogel sensors are biocompatible and biodegradable,[27] making them an attractive sustainable alternative to organic polymer materials derived from petroleum.

The utilization of proteins in organic solvents has numerous applications such as for the synthesis of pharmaceuticals, specialty chemicals, and biofuels,[28−30] as well as in the defense and environmental industries for sensing and degrading hazardous compounds.[31] Organic solvents generally deactivate protein function, i.e., ligand binding or catalysis. Organic solvents disrupt the protein−solvent interactions that drive polypeptide folding and control protein secondary and tertiary structures, causing denaturation of the native protein conformation.[32] Protein function is intimately linked to its highly specific three-dimensional conformation, where even slight perturbations from its native structure can have a large impact on the protein's functionality.[33] The protein's conformational flexibility may also decrease in an organic solvent by disrupting the solvation shell waters at the protein interface.[30,32,34−36] Numerous approaches have attempted to improve protein function in organic solvents; these methods include immobilizing proteins by cross-linking them to either other proteins or to other support materials such as silica or polymers, or by encapsulating the protein within other materials.[35,37−40]

Immobilized proteins often show higher activities in harsh environments compared to proteins free in solution. The protein secondary and tertiary structures of immobilized proteins are stabilized due to the accompanying increase in activation barriers for protein denaturation.[41,42] The subunits of immobilized multimeric proteins are also less likely to dissociate.[43,44] Additionally, proteins immobilized within hydrophilic polymers create favorable microenvironments containing the solvation shell waters that contribute to protein flexibility.[38,39,45]

Protein−protein cross-linking has been utilized for decades as a stabilization technique. For example, cross-linked enzymes (CLEs) were developed in the 1960s.[46] Subsequently, cross-linked enzyme crystals (CLECs)[47] were commercialized by Altus Biologics.[43] Cross-linked enzyme aggregates (CLEAs) were developed decades later to overcome the need for enzyme crystallization prior to cross-linking.[38,43] CLEAs are produced by adding a small concentration of a denaturant such as ammonium sulfate or an organic solvent to force protein aggregation. Then, a cross-linking agent, commonly glutaraldehyde, is added to cross-link the proteins within the aggregate. These cross-linked enzyme systems exhibit high protein activity in organic solvents.[42,48] However, the resulting microscopic enzyme particulates (5−50 μm) still require time-consuming separation processes that impede their recovery and reuse.

In the work here, we discuss the development of revolutionary responsive pure protein organogels. These pure protein polymer materials are fabricated by first cross-linking proteins in aqueous solutions to form protein hydrogels and do not require crystallization or aggregation of the proteins prior to cross-linking. Denaturants that induce protein aggregation and the subsequent glutaraldehyde cross-linking can decrease the enzymatic activity of the CLEA in water to 40−60% of the native-free enzyme.[49,50]

We demonstrate the utility of our protein organogels for chemical sensing and for enzyme catalysis. Large protein organogel films were fabricated by performing a stepwise solvent exchange on pure protein hydrogels to replace the aqueous solvent with pure ethylene glycol (EG), a low vapor pressure organic solvent (0.06 mm Hg at 20 °C). We show that our protein organogels retain substantial native protein functionalities such as selective ligand binding and enzymatic activity. The development of our 2DPC organogel sensors enables the detection of protein−ligand binding in nonaqueous environments. To the best of our knowledge, this is the first report of a pure protein organogel that exhibits a chemoselective VPT. Our catalytic protein organogels that utilize the enzyme organophosphorus hydrolase (OPH) to hydrolyze organophosphate nerve agents exhibit higher enzymatic activity in organic solvents relative to that of the native uncross-linked enzyme in an organic solvent. Dispersions of these biocatalytic hydrogel and organogel films could be used for both personal and large-scale decontamination of environmental toxins.

EXPERIMENTAL SECTION

Materials. Proteins, such as bovine serum albumin (BSA) (>98%; lyophilized powder, essentially fatty acid (FA)-free, CAS: 9048-46-8), were purchased from Sigma-Aldrich and dissolved in nanopure water at a concentration of 200 mg/mL prior to use. Ibuprofen sodium salt, Sigma-cote, NaOH pellets, sodium dodecanoate, sodium myristate, and $CoCl_2$ were purchased from Sigma-Aldrich and used as received. Glutaraldehyde (50 wt % in water) was purchased from Sigma-Aldrich and diluted with nanopure water to make a 12.5 wt % glutaraldehyde solution. Ethylene glycol was purchased from Fisher Scientific and used as received. The recombinant organophosphorus hydrolase (OPH) (EC 8.1.3.1; 72 kDa) mutant enzyme from *Pseudomonas diminuta* was produced in *Escherichia coli* at FLIR Systems Inc. The OPH solution contained 5.6 mg OPH/mL in a 0.01 M 4-(2-hydroxyethyl)-1-piperazineethanesulfonic acid (HEPES) buffer with a 100 μM $CoCl_2$ cofactor at pH 8. Ethyl-paraoxon (99.9%) was purchased from Chem Service, Inc., diluted with methanol to make a 152 mM paraoxon solution, and stored at 4° C in nanopure water.

Fabrication of Protein Organogels. Two pure protein organogels were fabricated for this study. One contained the transport protein BSA, while the other contained the enzyme OPH. Protein hydrogels were fabricated, followed by a stepwise solvent exchange procedure that transformed the protein hydrogels into protein organogels.

Fabrication of BSA Hydrogels and Organogel. BSA hydrogels were fabricated first by polymerizing 200 mg/mL BSA solutions 200 mg/mL BSA solutions between two between two glass slides using

DOI: 10.1021/acsami.9b18191
ACS Appl. Mater. Interfaces 2020, 12, 238−249

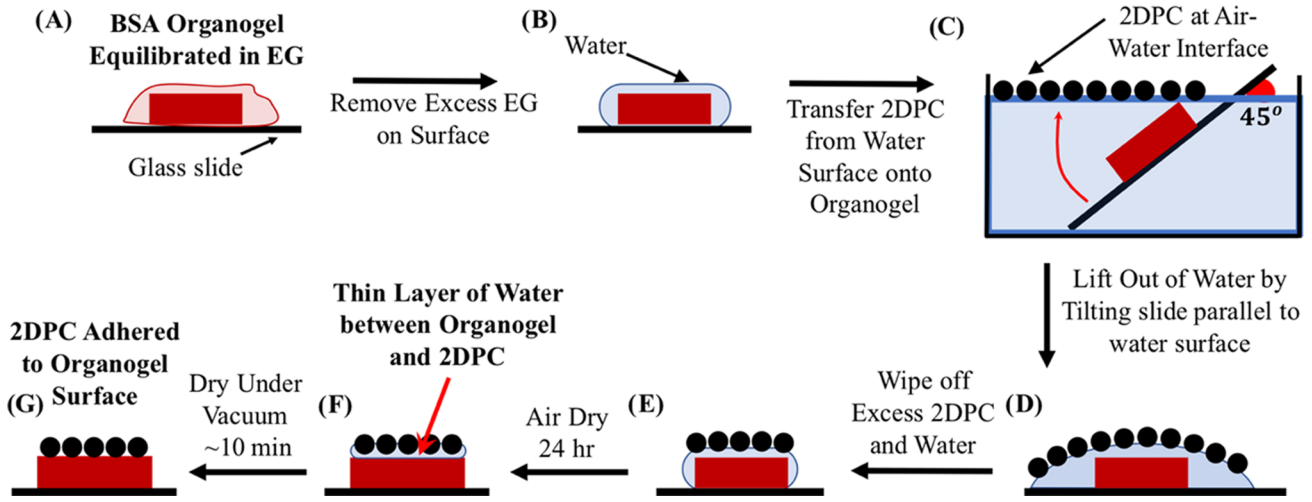

Figure 1. Attachment of 2DPC to BSA organogels after EG solvent exchange. (A) Organogel equilibrated in pure EG placed on a glass slide. (B) Organogel rinsed with a stream of nanopure water to exchange EG on the surface with water. (C) 2DPC is transferred from the air−water interface onto the organogel, as previously described.[69] (D) Slide and organogel are covered by a water layer with the 2DPC at the air−water interface. (E) Excess 2DPC and water are removed from around the organogel with a filter paper. (F) Allow the wet organogel to dry in ambient conditions for 24 h to evaporate most of the water layer. (G) Organogel is further dried under a decreased pressure (0.6 atm) for ~10 min, attaching the 2DPC to the organogel surface.

glutaraldehyde as the cross-linker, as described previously.[5] Glass slides were treated with Sigma-cote so that the glass slide surface was hydrophobic. Scotch tape was layered along the four edges of the slide to create a 410 μm thick spacer (measured using a digital micrometer with 10 μm precision). A 64 μL aliquot of a 12.5 wt % glutaraldehyde solution was added to 1 mL of the 200 mg/mL BSA solution. This solution was polymerized between the slides for 3 h at room temperature. The resulting transparent yellow pure BSA hydrogel films contained 15 vol % BSA. The hydrogel films were cut into square pieces. The dimensions of each piece were measured using a digital micrometer before being washed with nanopure H_2O for 48 h to remove unreacted glutaraldehyde and BSA.

The BSA hydrogels then underwent a stepwise solvent exchange that replaced the aqueous mobile phase with an organic solvent. We used EG as the organic solvent. EG is miscible with water and has a vapor pressure of 0.06 mm Hg at 20 °C. The dimensions of the BSA hydrogel pieces, equilibrated in nanopure water, were measured before the solvent exchange process. Samples were then incubated in 250 mL of a 30 vol % EG aqueous solution for 24 h, followed by incubation in 250 mL of 50 vol % EG for 24 h, and then incubated in 250 mL of 70 vol % EG for 24 h. Finally, the samples were equilibrated in pure EG solutions for 48−72 h, during which the EG solvent was replaced twice a day to remove nearly all of the water from the system. The BSA protein polymer most likely retains some solvation shell waters because these water layers are effectively bound to the proteins and difficult to exchange from the organogel network.

The dimensions of the square BSA hydrogel films were measured using the digital micrometer after equilibrating at each EG concentration. The volume fraction of BSA in the organogel samples equilibrated in each solvent mixture was calculated using the volume swelling ratio, $Q = (A_f/A_i)^{3/2}$, where A_i and A_f are the areas of the hydrogel/organogel square directly after polymerization and after equilibrating in the solvent mixture, respectively. The volume fraction of BSA in the hydrogel after polymerization is equal to that of the 200 mg/mL BSA solution, ~0.15 vol. fraction BSA. The vol. fraction of BSA in the organogel can thus be calculated as volume fraction $BSA_{organogel} = 0.15/Q$.

Fabrication of OPH Hydrogels and Organogels. The OPH enzyme, provided by FLIR Systems Inc., was received as a 5.6 mg/mL OPH solution in a 0.01 M HEPES buffer with 100 μM $CoCl_2$ at pH 8. For fabricating OPH hydrogels, the dilute OPH solution was first concentrated to ~200 mg/mL using Millipore Amicon 30 kDa centrifuge filters. The absorption at 280 nm was measured using a Cary 5000 UV−vis spectrometer. We calculated the OPH concentration using the Beer−Lambert equation. The molar extinction coefficient for the OPH mutant was experimentally determined by FLIR Systems Inc., $\varepsilon_{280\ nm} = 28\,290\ M^{-1}\ cm^{-1}$.

Polymerization of the concentrated OPH solution was initiated by adding 24 μL of 5 wt % glutaraldehyde to 400 μL of the 200 mg OPH/mL solution. The OPH was polymerized between two glass slides separated by a spacer of six layers of tape for 2 h at room temperature. The resulting 360 μm thick OPH hydrogel films were washed with pH 8, 100 μM $CoCl_2$, 0.01 M HEPES buffer for 48 h to remove unreacted glutaraldehyde and OPH. The OPH concentration in the hydrogel was ~200 mg/mL.

OPH organogels were fabricated using the same stepwise solvent exchange process as described for the BSA organogels. However, the OPH enzymes, as well as other metalloenzymes,[51] require an excess of the cofactor, Co^{2+} for maximum activity.[52] The activity of OPH is maximized in basic solutions;[19] the solutions were adjusted to pH ~ 8. Aqueous EG solutions containing 30, 50, and 70% EG were made by mixing HEPES buffer that contained $CoCl_2$ $CoCl_2$ with pure EG such that the final concentration in the solution contained 100 μM $CoCl_2$ and a 0.01 M HEPES buffer. The pH was adjusted to 8 by the addition of solid NaOH. Solid $CoCl_2$ and NaOH were directly dissolved into EG for the 100% EG solutions such that the final pure EG solution contained 100 μM $CoCl_2$ at pH 8.

Fabrication of 2D Photonic Crystal Protein Hydrogels and Organogels. Anionic monodisperse polystyrene spheres (1150 nm diameter) were synthesized via a dispersion polymerization method.[53] The 2DPCs are fabricated by the self-assembly of the charged particles at the air−water interface using the needle tip-flow self-assembly method developed by us.[54,55] The needle tip-flow method forms a highly ordered close-packed particle array at the air−water interface, which is easily transferred to a solid support such as a glass slide.[55] 2DPC BSA hydrogels were fabricated by polymerizing the BSA solution on top of a close-packed 2DPC, which embeds the particles on the hydrogel surface, as previously described.[5] We attach 2DPC to the organogel surface after the solvent exchange to pure EG because, otherwise, the VPT induced by solvent exchange would disorder the close-packed 2DPC particles.

The 2DPC was attached to the surface of BSA organogels equilibrated in pure EG for 48 h, as shown in Figure 1. First, the organogel film was placed on a glass microscope slide. The organogel on the slide has a thick layer of EG surrounding it. Excess EG on the slide and organogel surface was removed by flushing the surface with a

DOI: 10.1021/acsami.9b18191
ACS Appl. Mater. Interfaces 2020, 12, 238−249

stream of nanopure water. A thick layer of EG surrounding the organogel impedes 2DPC attachment. Replacing the EG on the organogel surface with water creates a more hydrophilic interface for the 2DPC transfer from the air−water interface. A 2DPC transferred from an air−water interface to a hydrophobic substrate tends to roll off the hydrophobic surfaces, similar to how droplets of pure water tend to roll off a hydrophobic surface. This results in a nonuniform coating of the 2DPC on the hydrophobic substrate. Additionally, removing the thick EG coating decreases the drying time after 2DPC transfer.

EG and water are miscible solvents, and inevitably some water will diffuse into the organogel when the EG is washed from its surface. The minor addition of water does not swell the organogel. Any water that diffuses into the organogel during the 2DPC attachment is removed when the 2DPC organogel is re-equilibrated in pure EG.

Flushing with water removes EG from the organogel surface and leaves a layer of water around the organogel interface, effectively creating a more hydrophilic surface for the 2DPC transfer (Figure 1B). The 2DPC particle array at the air−water interface was subsequently transferred onto the organogel surface, shown in Figure 1C,D. The procedure to transfer the 2DPC from the air−water interface to the organogel surface was discussed in detail previously.[55]

The EG inside the organogel has a low vapor pressure. The water layer between the 2DPC and the organogel, shown in Figure 1E, will preferentially evaporate before the EG solvating the organogel. The 2DPC BSA organogels are dried in air for 24 h to allow most of the water to evaporate. Further drying is required to decrease the water content and promote adhesion of the 2DPC to the organogel. The remaining water is removed by drying the 2DPC organogels in a vacuum oven under reduced pressure (0.6 atm) for 10−15 min at room temperature. After additional drying under reduced pressure, the 2DPC particles adhere to the organogel surface. The 2DPC organogels are then re-equilibrated in 250 mL of pure EG for 48 h.

2DPC BSA Organogel VPT Response to Ligand Binding. We monitored the volume response of the 2DPC BSA hydrogels and organogels to protein−ligand binding by measuring the particle spacing of the attached 2DPC. The 2DPC particle spacing, a, was calculated from the Debye ring diffraction measurements as previously described.[6,55] The hydrogel and organogel volume responses to ligand binding are plotted as the 2DPC particle spacings changes. The 2DPC particle spacing change is calculated as $\Delta a = a_{ligand} - a_{initial}$, where $a_{initial}$ is the 2DPC particle spacing of the BSA gel in equilibrium with its respective mobile phase and a_{ligand} is the 2DPC particle spacing of the BSA gel after 24 h exposure to solutions containing the ligand. The particle spacings of three 2DPC BSA gel samples were measured for each ligand concentration. The BSA ligands examined were ibuprofen and the two fatty acids (FAs), sodium dodecanoate, a C12 FA, and sodium myristate, a C14 FA. The linear best-fit lines were calculated using a weighted least-squares analysis. Normalized residual plots were also produced to validate the fit. Details of the weighted least-squares fit and the residual plots for each ligand are provided in the Supporting Information.

For the Ibuprofen experiments, the BSA hydrogels were equilibrated in 50 mM phosphate buffer pH 7.2. BSA organogels were equilibrated in either pure EG or 50 mM NaCl in the EG solution. The particle spacing was measured after the hydrogels and organogels equilibrated in the appropriate mobile phase for 24 h. BSA hydrogels were then incubated in 50 mM phosphate buffer containing 0, 1, 5, 10, 15, and 20 mM ibuprofen for 24 h. BSA organogels were incubated in either pure EG or 50 mM NaCl in the EG solution containing 0, 1, 5, 10, 15, 20, and 25 mM ibuprofen. The 2DPC particle spacing was measured after the samples were incubated in ibuprofen solutions for 24 h.

BSA is a highly promiscuous protein that binds many different ligands. Negative controls were performed using concanavalin A (ConA) and lysozyme organogels, which do not bind ibuprofen because a ligand that does not bind to BSA could not easily be found. Details of the ConA and lysozyme organogel fabrication are provided in the Supporting Information. The 2DPC particle spacing of these negative control organogels were measured before and after they were incubated in an EG solution containing 20 mM ibuprofen for 24 h.

The pK_a of fatty acids increase as the hydrocarbon tail length increases;[56] therefore, BSA hydrogels were equilibrated in a 50 mM carbonate−bicarbonate buffer at pH 9, and BSA organogels were equilibrated in EG solutions containing 10^{-5} M NaOH (EG ~ pH 9) to ensure that most FA molecules are ionized in solution. The C12 and C14 FAs have very low solubilities in water. We could obtain 5 mM dodecanoate (C12) solutions in 50 mM pH 9 buffer; however, the myristate (C14) FA was insoluble in buffer at 1 mM FA. Thus, the 2DPC particle spacings of BSA hydrogels were measured only for C12 FA solutions containing 0, 1, 2.5, and 5 mM C12 FAs.

Both the C12 and C14 FAs were readily soluble in pure EG and EG pH 9 solutions. The 2DPC particle spacings of BSA organogels were measured after 24 h exposure to 0, 1, 5, 10, 15, 20, and 25 mM FAs in EG pH 9 for both the C12 and C14 FAs.

Enzyme Activity Measurements of OPH Hydrogels and Organogels. The organophosphate, paraoxon, is used as the substrate to measure the OPH specific activity of OPH solutions, hydrogels, and organogels. Hydrolysis of paraoxon by OPH was monitored through the production of *p*-nitrophenol (pNP), which absorbs at 405 nm. The time dependence of the increasing absorbance at 405 nm for the OPH−paraoxon solutions was measured using a Cary 5000 UV−vis spectrometer. A 2 mm path length quartz cuvette was used for OPH solution measurements, and a 10 mm path length quartz cuvette was used for the hydrogel and organogel measurements.

The 5.6 mg/mL OPH solution from FLIR was diluted with either water or an EG/water mixture to a concentration of 2.8×10^{-4} mg/mL for the OPH monomer samples. The OPH gel films were cut into roughly 0.5 mm × 0.5 mm pieces so that the OPH concentration in the 4 mL cuvette volume was ~2.8×10^{-4} mg/mL. The 0.036 mm thick OPH hydrogel and organogel films contain 200 mg of OPH per mL of gel. Each piece of OPH gel was measured with a digital micrometer, and the weight of OPH, mg_{OPH}, was calculated for each hydrogel or organogel sample. As a control, the supernatant buffer solution from OPH hydrogel samples was also measured. OPH hydrogels were separated from the buffer by centrifugation at 5000 rpm for 5 min. The specific activity of the supernatant was calculated to determine if any OPH monomer remained in the supernatant.

A stock solution of paraoxon was added to each sample so that the final concentration was 1.5 mM paraoxon. The 15 mM paraoxon stock solution contained 10% ethanol in water to increase the paraoxon solubility in water. A 100 μL aliquot of paraoxon stock solution was added to 1 mL of the OPH monomer solution and the hydrogel supernatant solution. A 400 μL aliquot of paraoxon stock solution was added to the 4 mL samples containing the OPH hydrogel and organogel samples. After the addition of paraoxon, the samples were very quickly moved to the spectrometer where the absorbance at 405 nm was measured every 30 s for 5 min. The solutions were stirred between absorbance measurements to facilitate the diffusion of paraoxon to the OPH gel, which rests at the bottom of the cuvette. Measurements were performed in triplicate.

We calculated the OPH specific activity in units of the molarity of pNP produced per mg of OPH with time: $(M_{pNP})/(\text{min}*mg_{OPH})$ from the evolution of the absorption at 405 nm over several minutes. The slope of the line, $\Delta absorbance/\Delta time$, is determined for each sample and used to calculate the OPH specific activity using (eq 1). The molar extinction coefficient, ε, of *p*-nitrophenol in alkaline conditions is 17 100 M^{-1} cm^{-1}. The path length, *b*, was 0.2 cm for OPH solution measurements and 1 cm for OPH hydrogel and organogel measurements. The OPH concentration, [OPH], in the hydrogel and organogel samples was calculated from the gel size as described in the previous paragraphs for each calculation

$$\text{activity} = \frac{\text{slope}}{\varepsilon * b * [\text{OPH}]} \quad (1)$$

DOI: 10.1021/acsami.9b18191
ACS Appl. Mater. Interfaces 2020, 12, 238−249

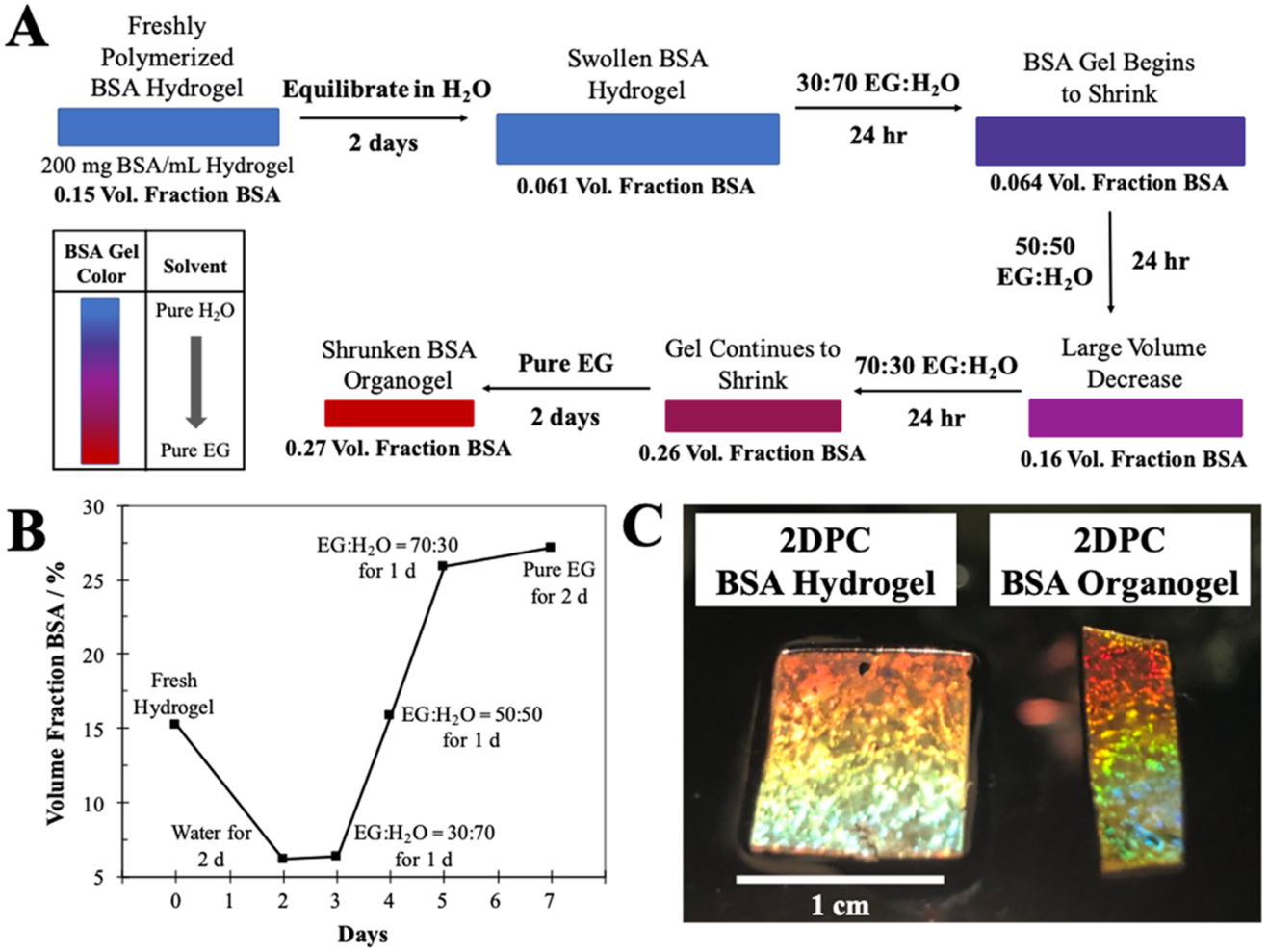

Figure 2. (A) Schematic showing a stepwise solvent exchange procedure that transforms BSA hydrogels into BSA organogels in pure EG. (B) Volume fraction of BSA in the gel is calculated from the swelling ratio after each stage of the stepwise solvent exchange process. (C) Photograph of a 2DPC BSA hydrogel film and a 2DPC BSA organogel film. Both the hydrogel and organogel show intense 2DPC diffraction of visible light. The image illustrates the bright diffraction that results from forward scattered light for the 2DPC BSA gel films lying flat on a glass slide. The flashlight was placed behind the sample such that the intense forward diffracted light is recorded. The 2DPC hydrogel and 2DPC organogel diffract different color patterns because the two gels have different 2DPC particle spacings.

RESULTS AND DISCUSSION

Fabrication of Functional Pure Protein Organogels from Pure Protein Hydrogels. Pure protein hydrogels were fabricated by cross-linking the protein lysine groups using glutaraldehyde.[5,21] We previously demonstrated that this mild glutaraldehyde cross-linking method results in the formation of transparent hydrogels that undergo VPT in responses to protein−ligand binding for the proteins bovine and human serum albumin, glucose binding protein, and concanavalin A.[5,24,25] These fabricated pure protein hydrogels are robust macroscopic films. We have fabricated pure protein hydrogels as large as 4 cm × 7 cm and believe that this process can be easily scaled up much further.

Proteins evolved to function mainly in aqueous solvents, where interactions between amino acid side chains and water are important for protein folding and dynamics.[32] Thus, we expected that these glutaraldehyde cross-linked hydrogel proteins would retain their native protein monomer structures and functions. Somewhat surprisingly, the organogel proteins also retain a significant portion of their native protein monomer function, enabling revolutionary applications of pure protein sensors and catalysts. An organic solvent mobile phase hinders the growth of microbes that would digest the proteins, therefore increasing the shelf life of the pure protein organogels compared to that of the protein hydrogels. We have observed a significant degradation of our pure protein hydrogels by microbes after a week at room temperature, whereas we do not observe such degradation in the organogels after more than 3 months. The solubility of hydrophobic analytes increases in organic solvents, enabling the use of protein organogel sensors and biocatalysts for detecting or catalyzing reactions of hydrophobic species, such as organophosphates, polychlorinated biphenyls, and many volatile organic compounds such as toluene. The utilization of enzyme chemistry in pure organic solvents is also highly important in the pharmaceutical industry. The organic mobile phases can promote enhanced enantioselectivity of the substrate and/or products and enable novel enzymatic transformations such as reverse hydrolysis of alcohols to esters because water-dependent reactions are disabled.[29]

Our responsive pure protein organogels are fabricated by performing a stepwise solvent exchange on pure protein hydrogels, as shown in Figure 2A. The protein cross-linking that forms the hydrogel network effectively immobilizes the

DOI: 10.1021/acsami.9b18191
ACS Appl. Mater. Interfaces 2020, 12, 238−249

proteins prior to their exposure to organic solvent. Protein immobilization increases protein stability against thermal and chemical denaturation.[41,43] This method of fabricating protein organogels seems to be universal with respect to the protein identity, producing transparent and mechanically stable protein organogel films for each protein tested. We successfully fabricated many protein organogels, including bovine/human serum albumin (BSA/HSA), organophosphorus hydrolase (OPH), Concanavalin A, lysozyme, and myoglobin. Similar to protein immobilization onto a solid matrix, our macroscopic protein hydrogel and organogel films enhance the recovery and reuse of the proteins and enable their use in continuous operations such as fixed-bed reactors.[42,57]

By utilizing the low vapor pressure organic solvent, EG, we create responsive pure protein organogels that resist mobile phase evaporation. The mobile phase is essential for the 2DPC sensor VPT response to ligand binding; the VPT volume change is the result of an osmotic pressure within the protein polymer system that triggers mass transport of the mobile phase. For example, VPT swelling in response to an analyte is not possible in the absence of a mobile phase because swelling is caused by solvent repartitioning within the polymer network. A low vapor pressure mobile phase increases the sensor operational time and enhances its potential applications. Additionally, mobile phase evaporation can limit the diffusion of species to the protein active sites, therefore decreasing the sensor and/or catalyst kinetics.

We first characterized the solvent-exchange-induced VPT that transforms our protein hydrogels into protein organogels.

Much of our initial organogel work utilized the inexpensive and ubiquitous protein BSA. As shown in Figure 2A, the BSA hydrogels undergo a VPT that significantly shrinks the system as the EG concentration increases.

We quantitatively monitor this VPT by calculating the BSA volume fraction at each EG concentration using the swelling ratio, Q (Figure 2B). The BSA volume fractions in the hydrogel and organogel are proportional to the gel volume, increasing or decreasing when the protein polymer shrinks or swells. Calculating the BSA volume fraction from the swelling ratio is possible because the initial BSA volume fraction is known; the freshly polymerized BSA hydrogel contains 200 mg/mL BSA, which corresponds to a BSA volume fraction of 15%.

As shown in Figure 2B, the initially polymerized BSA hydrogels swell upon equilibration in nanopure water. The resulting BSA volume fraction decreases to 6.1%. The BSA volume fraction increases during the stepwise EG exchange toward pure EG to a maximum volume fraction of 27% BSA after equilibrating in pure EG after 2 days.

Fabrication of 2DPC Protein Organogels. We recently developed several 2DPC hydrogel sensors for multiple analytes.[6,24,25] The 2DPC consists of a well-ordered hexagonal array of nanoparticles with particle spacings comparable to the wavelengths of visible light. The 2DPC diffracts visible light according to the 2D Bragg diffraction equation.[55] The 2DPC simultaneously diffracts these wavelengths of light into multiple angles to produce the rainbow patterns observed in Figure 2C. When monochromatic incident light is normal to the 2DPC, the diffraction produces a Debye ring that has a diameter corresponding to the diffraction angle.[55] These wavelength-dependent diffraction angles are determined by the 2DPC particle spacings, and the intensity of this diffraction depends on the 2DPC particle ordering.[55] Hydrogel volume changes induced by analyte binding alter the 2DPC particle spacings and shift the diffraction angles. Thus, these shifts in the diffraction angle monitor the hydrogel VPT and report on the analyte concentration.

The 2DPC particles are close-packed when fabricated.[55] For hydrogels, this close-packed particle array is embedded in the hydrogel surface during polymerization. Generally, hydrogels swell upon exposure to aqueous solutions after they are polymerized, increasing the 2DPC particle spacing, as is the case for the BSA hydrogels in water. The solvent-exchange-induced VPT, shown in Figure 2B, significantly shrinks the protein hydrogel/organogel. The organogel BSA volume fraction is roughly twice that of the initially polymerized protein hydrogel. Thus, the close-packed 2DPC that was initially attached to the hydrogel during polymerization will disorder during the solvent exchange when it attempts to decrease the particle spacing to less than the close-packed particle spacing.

To avoid 2DPC disordering, we attached the 2DPC to the organogel after EG solvent exchange. This enables the 2DPC diffraction measurements to monitor organogel swelling induced by ligand binding. 2DPC diffraction measurements are a much more sensitive monitor of organogel volume changes than physically measuring the dimensions of the organogel film.

Functional Pure Protein Organogel Sensors and Enzymatic Catalysts. We fabricated pure protein organogels using two proteins with very different biological functions to demonstrate the versatility of our fabrication procedure and to highlight two different applications of these materials.

Our protein organogels retain a significant fraction of their native protein function because the proteins are immobilized during the protein hydrogel fabrication. This protein immobilization is critical for the preservation of protein function in our organogels. The glutaraldehyde cross-linking immobilizes the proteins by forming multiple covalent bonds between lysine residues on the protein surface. This immobilization stabilizes the native protein structure by increasing the activation barrier for protein unfolding,[42] creating a system where the proteins are more resistant to denaturation or deactivation by organic solvents. For multimeric proteins, such as the dimeric enzyme, OPH, discussed below, the immobilization also prevents subunit dissociation.

2DPC BSA Organogel Ligand Binding Sensor: Ibuprofen and Fatty Acids. Albumins are promiscuous proteins that bind many ligands and transport them throughout the body.[58−60] We previously developed 2DPC BSA hydrogel sensors that exhibit VPT in response to changes in the number of bound charges on the protein caused by pH changes and the binding of divalent metal ions, surfactants, fatty acids, and charged drug molecules.[5] We discovered that our 2DPC BSA organogels also exhibit VPT in response to BSA−ligand binding.

Figure 3 compares the 2DPC particle spacing change of BSA hydrogels and organogels in response to binding an ibuprofen salt and two fatty acids, sodium dodecanoate (C12 FA) and sodium myristate (C14 FA). Ibuprofen and the two FAs are more soluble in EG than in water, enabling the BSA organogels to sense larger ligand concentrations compared to the hydrogel. This increases the functional dynamic range of the sensor. This increase in dynamic range is most notable in the FA system; for example, the solubility of the C14 FA in pH 9

DOI: 10.1021/acsami.9b18191
ACS Appl. Mater. Interfaces 2020, 12, 238−249

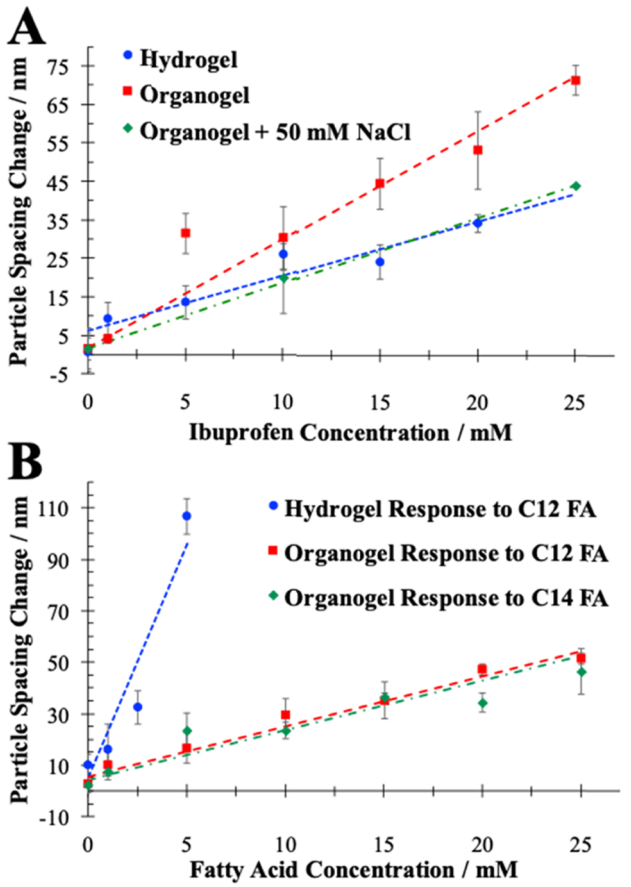

Figure 3. Average particle spacing changes of 2DPC BSA hydrogels and organogels as a function of ligand concentration. (A) Ligand:ibuprofen sodium salt. For the hydrogels, ibuprofen was dissolved in 50 mM phosphate buffer at pH 7.2. For the organogels, ibuprofen was dissolved in either pure EG or EG containing 50 mM NaCl. (B) Ligands: C12 and C14 fatty acids (FAs). For the hydrogels, C12 FA was dissolved in a 50 mM carbonate−bicarbonate buffer at pH 9. The C14 FA is not soluble in water at these concentrations. For organogels, C12 and C14 FAs were dissolved in EG pH 9. Error bars are 1 standard deviation. The linear best-fit lines were calculated using the weighted least-squares analysis.

buffer is less than 1 mM, whereas the solubility in EG is greater than 25 mM.

The particle spacing of both the 2DPC BSA hydrogels and organogels monotonically increases with increasing concentrations of ibuprofen (Figure 3A) and the FA (Figure 3B). The increasing particle spacing is caused by volume phase transitions (VPTs) that swell the hydrogels and organogels in response to the charged ligands binding to the cross-linked BSA proteins. Protein organogels fabricated using proteins that do not bind the ligands do not exhibit organogel volume changes. The results from these negative control experiments are shown in Figure SI 1 in the Supporting Information.

The linear best-fit lines in Figure 3 were calculated using the weighted least-squares method. The normalized residual plots (Figure SI 2 in the Supporting Information) demonstrate that 65% of the data points fall within 1 standard deviation and >90% of the data points fall within 2 standard deviations of the best-fit line. The Gaussian distribution of the data about the best-fit line validates that the 2DPC particle spacing change is linear with respect to the ligand concentrations tested.

Hydrogel and organogel VPT result from induced osmotic pressures, $\prod$, that cause translocation of the mobile phase. According to the Flory−Rehner−Tanaka theory,[16,17] these osmotic pressures are induced by changes in the total Gibbs free energy of the system, ΔG_{Total}. The resulting VPT causes the polymer network to either expel solvent, causing the system to shrink or to transport additional solvent into the polymer network, causing the system to swell until an equilibrium volume is reached where $\Pi_{Total} = \frac{\partial \Delta G_{Total}}{\partial V} = 0$.

The total Gibbs free-energy change in an ionic polymer network such as our BSA polymer has contributions from changes in the free energy of mixing, ΔG_{Mix}, changes in the free energy of elasticity, $\Delta G_{Elastic}$, and changes in the ionic free energy, ΔG_{Ion}.[12,17] At the equilibrium volume, the interactions between the polymer and solvent that contribute to the total Gibbs free energy are balanced. Thus, a reaction that disrupts this balance of interactions causes $\Delta G_{Total} \neq 0$, which subsequently actuates a volume change to relieve the osmotic pressure. The magnitude of the volume change is proportional to the magnitude of the change in the total Gibbs free energy.

The BSA hydrogel and organogel VPT that results from the protein binding charged ligands are measured using the 2DPC particle spacing changes, shown in Figure 3. These volume changes are caused by ΔG_{Ion} and ΔG_{Mix}. The free energy of mixing depends on the interactions between the BSA polymer and the mobile phase solvating the polymer. The significant difference between the hydrogel volume and the organogel volume, shown in Figure 2, indicates that there is a large initial difference prior to ligand binding in the polymer−solvent interactions between the BSA polymer and two mobile phases. Assuming that the degree of ligand ionization is constant, ΔG_{Ion} is directly correlated to the number of charges bound to the protein polymer network, the Donnan potential. ΔG_{Ion} is attenuated by increasing the mobile phase ionic strength.

We can directly observe this ionic strength attenuation in Figure 3A. The 2DPC organogel particle spacing change in response to ibuprofen in pure EG is larger than that of the hydrogel in 50 mM buffer. However, when 50 mM NaCl is added to EG such that the ionic strength of the EG is roughly equal to that of the buffer, the particle spacing changes for the hydrogel and organogel become similar. These results indicate that the hydrogel and organogel VPT in response to ibuprofen binding are primarily driven by ΔG_{Ion}. Since ΔG_{Ion} is directly proportional to the number of bound charges, we can also conclude that the binding affinities of the six ibuprofen binding sites in BSA[61] are roughly the same for the hydrogel and organogel systems. Our results also suggest that the ΔG_{Mix} caused by ibuprofen binding to the BSA polymer is similar for the hydrogel and organogel systems, due to the similar responses of the hydrogel in 50 mM buffer and the organogel in the 50 mM NaCl EG solution when the ionic strengths are roughly equal.

As shown in Figure SI 1 in the Supporting Information, our protein organogels exhibit VPT only when the protein−ligand binding occurs. The proteins ConA and lysozyme do not have ibuprofen binding sites like that of the BSA. Thus, the ConA and lysozyme organogels show negligible 2DPC particle spacing changes when incubated in EG solutions containing 20 mM ibuprofen, whereas the BSA organogels exhibit a ~55 nm 2DPC particle spacing change.

The 2DPC particle spacing change of BSA hydrogels and organogels in response to FA binding is shown in Figure 3B for

DOI: 10.1021/acsami.9b18191
ACS Appl. Mater. Interfaces 2020, 12, 238−249

the C12 FA, dodecanoate, and the C14 FA, myristate. The BSA organogel has a much larger functional dynamic range, enabling the organogel sensor to detect larger FA concentrations because the FAs have larger solubilities in EG. The C14 FA was insoluble in aqueous solutions at 1 mM concentrations. The C14 FA is highly soluble in EG such that a 25 mM C14 EG solution can be made. The ability of the BSA organogel sensors to detect molecules like the C14 FA that are practically insoluble in water clearly highlights one of the major advantages these BSA organogels have compared to the BSA hydrogels.

The 2DPC BSA hydrogel particle spacing change is much larger than that of the organogel at the same FA concentration despite the hydrogel system having higher ionic strength. These results indicate that either the binding affinities of the seven FA binding sites[58] on BSA decrease when the protein polymer is solvated by EG or that ΔG_{Mix} has a more significant contribution to ΔG_{Total} for the FA−BSA binding VPT response compared to that of ibuprofen.

Catalytic OPH Hydrogels and Organogels. Organophosphates (OP) are a class of highly toxic organic molecules used as pesticides and chemical warfare agents that cause >200 000 deaths per year.[62] Despite a ban on chemical weapons, OP nerve agents are continually used in attacks, such as in Syria, and political assassinations. Current commercial products used by the military for OP decontamination are often caustic due to the use of strong inorganic oxidizers such as hypochlorite or require preparation prior to use, which complicates their use in the field.[31]

Some species of bacteria and fungi have evolved enzymes, like OPH, that hydrolyze the phosphoester bond of OP, creating less toxic products.[63] These enzymes are highly efficient catalysts that generally hydrolyze numerous OP compounds such as paraoxon, parathion, sarin, VX, and soman. Enzymatic decontamination solutions generally operate under mild conditions that are appropriate for personal and/or sensitive material decontamination; however, the use of enzymes in harsher conditions is limited by their stability. Practical utilization of enzyme-based decontamination solutions requires the stabilization of the enzymes to increase their shelf life and operational conditions and functional lifetime.

Our goal is to create simple decontamination systems that are appropriate for many potential applications such as personal decontamination for war-fighters and victims, large-scale decontamination of OP residues on surfaces, and for OP stockpile elimination. We envision a sprayable decontamination solution that can be easily and quickly applied to contaminated surfaces and skin. This would be accomplished by formulating a dispersion of our OPH hydrogel or organogel flakes in appropriate mobile phases.

An aqueous dispersion of our OPH hydrogel system would function as a potentially nontoxic, biodegradable solution that could be used on the skin and for sensitive materials where evaporation of water is not a concern. The OPH enzymes are immobilized via cross-linking to form the hydrogel network. Immobilized enzymes are typically stabilized with respect to time, which increases the shelf life of the immobilized enzyme material compared to their monomers in solution.[64] This stabilization enhances the usefulness of these materials. However, evaporation of the hydrogel aqueous mobile phase limits their application for large-area decontamination in hot, dry environments.

Our OPH organogels that utilize the low vapor pressure mobile phase, ethylene glycol, surmount some of the limitations of hydrogel materials such as evaporation. These low vapor pressure OPH organogel materials can be utilized for large-scale decontamination applications after a chemical weapon attack, for example, because the mobile phase resists evaporation. This allows for stand-off applications of the OPH organogel dispersion, where it can be sprayed over large areas from long distances without risk to the user. Preserving the mobile phase for a longer time also enables the diffusion of the OPH organogel flake dispersion into porous materials such as soil and affords the materials a longer working time to ensure complete hydrolysis of the dangerous OP molecules residing on the surfaces of streets and buildings.

OPH organogels can also be utilized to neutralize stockpiles of bulk nerve agents. Stockpiles consist of concentrated OP solutions in organic solvents. OP nerve agents are stored in organic solvents because they have limited solubility in water.[65] Un-cross-linked OPH monomers are not effective solutions for neutralizing these stockpiles because the enzymes are inhibited by the presence of the organic solvents.[66] The immobilized OPH in the organogel retains much of its native enzyme activity in the organic solvent, enabling OPH organogel neutralization of OP stockpiles. An additional advantage of these macroscopic OPH organogel films is that they can easily be separated from the stockpile solutions after OP hydrolysis and reused.

Biocatalytic pure protein hydrogels and organogels were fabricated using the enzyme organophosphorus hydrolase (OPH) provided by FLIR Systems Inc. OPH is a dimeric metalloenzyme that catalyzes the hydrolysis of various OPs.[8,66] We examined the hydrolysis of the OP, ethyl-paraoxon, a commonly used nerve gas simulant. OPH is a remarkably efficient enzyme, having a nearly diffusion-limited hydrolysis rate.[63] Ethyl-paraoxon is hydrolyzed by OPH in the presence of the cofactor, Co^{2+}, to produce *p*-nitrophenol (pNP), diethylphosphate, and two protons (Figure 4A). The rate of OP hydrolysis is easily measured from the increasing concentration of the hydrolysis product, pNP, which strongly absorbs 405 nm light under alkaline conditions.

We used the methods described above to fabricate OPH hydrogels and organogels. The specific activities of OPH monomer solutions and OPH hydrogels are shown in Figure 4B. Glutaraldehyde cross-linked OPH hydrogels retain 86% of their native enzymatic activity. The modest reduction in the OPH activity after immobilization compared to that of the OPH monomer is comparable to that of other immobilized enzymes in aqueous solutions.[67] The supernatant buffer solution separated from the OPH hydrogel by centrifugation exhibits insignificant OPH activity. This demonstrates that OPH irreversibly cross-links into the protein polymer and does not leach from the hydrogel. The specific activity calculated for the OPH hydrogel stems solely from the cross-linked OPH hydrogel.

The OPH enzyme monomers are typically deactivated by organic solvents. The specific activity of the un-cross-linked OPH monomers drastically decreases with increasing concentrations of EG (Figure 4B). In 50 vol % EG in water, the OPH monomer only retains 0.2% of the native OPH activity. The negative effects of organic solvents on the OPH activity were documented for other water−organic solvent mixtures; OPH was inhibited by 50% in aqueous mixtures containing 0.5% of common organic solvents like ethanol and isopropanol.[66]

DOI: 10.1021/acsami.9b18191
ACS Appl. Mater. Interfaces 2020, 12, 238−249

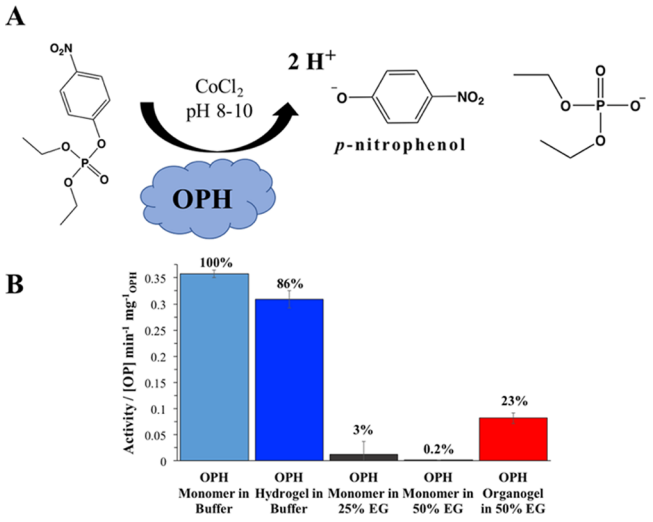

Figure 4. (A) Hydrolysis of ethyl-paraoxon by OPH enzyme in pH 8 HEPES buffer solution containing the cofactor, 100 μM Co^{2+}. (B) Specific activities for OPH monomer in buffer solution and EG-buffer solutions, the OPH hydrogel in buffer, and the OPH organogel in 50% EG-buffer solution.

The immobilized OPH in our organogels is less inhibited by the presence of a deactivating organic solvent than the free OPH monomer (Figure 4B). The organogel OPH retains 23% of the native OPH monomer activity in 50 vol % EG, whereas the OPH monomer is inactive in 50 vol % EG. Our OPH organogel exhibits a ~160-fold increase in enzymatic activity compared to the OPH monomer activity in 50% EG−water, as shown in Figure 4B. The activity enhancement of immobilized enzymes compared to that of free enzymes in organic solvents varies, depending on the immobilization technique, the enzyme, and the organic solvent properties. The 160-fold increase in activity exhibited by our OPH organogels relative to that of the OPH monomer is comparable to activity enhancements exhibited by other immobilized enzymes.[35,67] For example, the activity of α-chymotrypsin immobilized on nanoporous silica particles showed a 65-fold increase in isooctane and acetonitrile, a 110-fold increase in hexane, and a 1000-fold increase in methanol when compared to that of the free enzyme in those solvents.[68] Immobilization of catalase and horse liver alcohol dehydrogenase on microcrystals resulted in a 25-fold (catalase) and 50-fold (alcohol dehydrogenase) activity enhancement compared to that of their free enzyme activities in >95% propanol solutions.[69]

The enhanced activity of these OPH organogels in EG/water solutions most likely results from the glutaraldehyde cross-linking that immobilizes the enzymes. Glutaraldehyde cross-linking of OPH lysine residues potentially creates four covalent bonds at the four reactive lysine residues on the surface of OPH,[63] thus immobilizing the dimeric enzymes with multiple covalent bonds to adjacent enzymes. This multipoint covalent immobilization stabilizes the OPH native structure and prevents dissociation of the two identical subunits.[37]

The continued utilization of OP as chemical weapons, assassination agents, and pesticides represents an extremely dangerous threat to our military, aid workers, and the public. The development of our OPH hydrogels and revolutionary OPH organogels significantly advances efforts toward producing improved OP decontamination solutions that can be utilized under harsh conditions such as in an organic solvent or in hot, dry environments where either the OPH monomers or the OPH hydrogels would have limited functionality. Our cross-linked OPH hydrogel and organogel materials, formulated as a dispersion of small organogel film flakes, represent a simple sprayable solution for OP decontamination. These OPH organogels improve upon existing inorganic-based OP decontamination solutions, in that they would not be corrosive to coatings and sensitive equipment.[31] Furthermore, the pure OPH polymer of the organogels offers revolutionary catalytic capabilities compared to materials where OPH is immobilized on solid substrates because every monomer is a catalytic functional group. A small piece of this OPH organogel film (1 × 1 × 0.04 cm^3) with 23% remaining activity can hydrolyze 1 μM (275 mg/m^3) of paraoxon per minute. Thus, just 1 mL of a 20 vol % dispersion of these flakes could decontaminate up to 5 μM (1.3 g/m^3) of paraoxon per minute.

The EPA acute exposure guideline levels provide guidance on dangerous nerve agent concentrations for a given exposure time. For the most commonly used nerve agent, sarin, the lethal concentrations for acute exposure range from 0.38 mg/m^3 Sarin (10 min exposure time) to 0.013 mg/m^3 sarin (24 h exposure time). Assuming our OPH organogels catalyze the hydrolysis of other OP molecules with roughly similar rates to those measured for paraoxon, the 1 mL aliquot of a 20 vol % OPH organogel dispersion would decontaminate a lethal, 10 min exposure, sarin dose in less than a second.

These proof-of-concept experiments demonstrate the potential of these easily produced macroscopic OPH organogel films to improve upon existing pure immobilized enzyme technologies. For instance, our large OPH organogel films are much easier to separate from the reaction medium and reuse compared to the 5−50 μm diameter OPH cross-linked enzyme crystal particulates.[70] Enzyme crystallization is not required for the fabrication of these enzyme organogels, thus increasing the number of enzymes that can be used to produce these pure enzyme organgels compared to the CLECs. Future publications will investigate the stability of the OPH organogel activity over time, determine the OPH organogel activity in pure EG, and investigate other organic solvents and enzymes.

CONCLUSIONS

We developed a simple approach to fabricating responsive pure protein organogels from their hydrogels and demonstrated valuable applications like sensing and catalysis. Our method for fabricating pure protein organogels can be extended to other enzymes and protein−ligand binding pairs. This approach is a general platform for developing pure protein functional organogels. A major advantage of the protein organogel system lies in its ability to utilize low vapor pressure organic liquids as a mobile phase that will not evaporate in ambient conditions. Furthermore, organic solvent mobile phases increase the solubility of hydrophobic compounds, increasing the functional dynamic range of our 2DPC sensors.

The BSA organogels bind the same ligands as the native protein. This ligand binding induces macroscopic volume phase transitions. Our BSA organogels act as sensors for protein−ligand binding and represent a novel sensing motif for quantitating ligand binding in nonaqueous solvents. An important future application may include the detection of fentanyl in drug samples, a dangerous opiate with limited water solubility.

Our OPH organogels act as catalysts for decontaminating toxic OP. OPH organogels retained significant activity toward

DOI: 10.1021/acsami.9b18191
ACS Appl. Mater. Interfaces 2020, 12, 238−249

the hydrolysis of paraoxon compared to the OPH monomer in the presence of organic solvents. For field applications, the organogels could be formulated into a sprayable dispersion of OPH organogel flakes in EG for large-area decontamination. Important future applications could include developing these catalytic organogels using enzymes that degrade additional chemical weapon agents like mustard gas or agent orange.

■ ASSOCIATED CONTENT

Supporting Information

The Supporting Information is available free of charge at https://pubs.acs.org/doi/10.1021/acsami.9b18191.

Fabrication of ConA and lysozyme organogels and their 2DPC organogel sensor particle spacing changes in response to Ibuprofen; weighted least-squares analysis of 2DPC particle spacing changes for BSA hydrogels and organogels; and the normalized residual plots from the calculated linear fits (PDF)

■ AUTHOR INFORMATION

Corresponding Author

*E-mail: asher@pitt.edu.

ORCID

Natasha L. Smith: 0000-0001-9308-5178

Sanford A. Asher: 0000-0003-1061-8747

Present Address

§School of Engineering and Applied Science, University of Virginia, Charlottesville, Virginia 22903, United States (V.G.).

Author Contributions

All authors have given approval to the final version of the manuscript.

Funding

This work was funded by the Defense Threat Reduction Agency under grant HDTRA1-15-1-0038.

Notes

The authors declare no competing financial interest.

■ ACKNOWLEDGMENTS

The authors acknowledge Dr. Mark Wendt from the University of Wisconsin Madison and Dr. Iván Pallares for providing their Chem 563 Physical Chemistry Lab course material. These materials were used to calculate the weighted least-squares analysis. The authors acknowledge the generosity of Jeremy Walker and David Wilson from FLIR Systems Inc. for providing them with the OPH enzyme.

■ ABBREVIATIONS

2DPC, 2-dimensional photonic crystal
VPT, volume phase transitions
C12 FA, dodecanoate
C14 FA, myristate
BSA, bovine serum albumin
OPH, organophosphorous hydrolase
OP, organophosphate
EG, ethylene glycol

■ REFERENCES

(1) Richter, A.; Bund, A.; Keller, M.; Arndt, K.-F. Characterization of a Microgravimetric Sensor Based on pH Sensitive Hydrogels. *Sens. Actuators, B* **2004**, *99*, 579−585.

(2) Kamenjicki Maurer, M.; Lednev, I. K.; Asher, S. A. Photoswitchable Spirobenzopyran-Based Photochemically Controlled Photonic Crystals. *Adv. Funct. Mater.* **2005**, *15*, 1401−1406.

(3) Xu, F.-J.; Kang, E.-T.; Neoh, K.-G. pH- and Temperature-Responsive Hydrogels from Crosslinked Triblock Copolymers Prepared via Consecutive Atom Transfer Radical Polymerizations. *Biomaterials* **2006**, *27*, 2787−2797.

(4) Walker, J. P.; Asher, S. A. Acetylcholinesterase-Based Organophosphate Nerve Agent Sensing Photonic Crystal. *Anal. Chem.* **2005**, *77*, 1596−1600.

(5) Cai, Z.; Zhang, J.-T.; Xue, F.; Hong, Z.; Punihaole, D.; Asher, S. A. 2D Photonic Crystal Protein Hydrogel Coulometer for Sensing Serum Albumin Ligand Binding. *Anal. Chem.* **2014**, *86*, 4840−4847.

(6) Cai, Z.; Smith, N. L.; Zhang, J.-T.; Asher, S. A. Two-Dimensional Photonic Crystal Chemical and Biomolecular Sensors. *Anal. Chem.* **2015**, *87*, 5013−5025.

(7) Lin, G.; Chang, S.; Kuo, C. H.; Magda, J.; Solzbacher, F. Free Swelling and Confined Smart Hydrogels for Applications in Chemomechanical Sensors for Physiological Monitoring. *Sens. Actuators, B* **2009**, *136*, 186−195.

(8) Lu, H. D.; Wheeldon, I. R.; Banta, S. Catalytic Biomaterials: Engineering Organophosphate Hydrolase to form Self-Assembling Enzymatic Hydrogels. *Protein Eng., Des. Sel.* **2010**, *23*, 559−566.

(9) Xu, X.; Xu, Z.; Yang, X.; He, Y.; Lin, R. Construction and Characterization of a Pure Protein Hydrogel for Drug Delivery Application. *Int. J. Biol. Macromol.* **2017**, *95*, 294−298.

(10) Dey, N.; Samanta, S. K.; Bhattacharya, S. Selective and Efficient Detection of Nitro-Aromatic Explosives in Multiple Media Including Water, Micelles, Organogel, and Solid Support. *ACS Appl. Mater. Interfaces* **2013**, *5*, 8394−8400.

(11) Mukhopadhyay, P.; Iwashita, Y.; Shirakawa, M.; Kawano, S.-i.; Fujita, N.; Shinkai, S. Spontaneous Colorimetric Sensing of the Positional Isomers of Dihydroxynaphthalene in a 1D Organogel Matrix. *Angew. Chem.* **2006**, *118*, 1622−1625.

(12) Goponenko, A. V.; Asher, S. A. Modeling of Stimulated Hydrogel Volume Changes in Photonic Crystal Pb2+ Sensing Materials. *J. Am. Chem. Soc.* **2005**, *127*, 10753−10759.

(13) Anees, P.; Praveen, V. K.; Kartha, K. K.; Ajayaghosh, A. 16—Self-Assembly in Sensor Nanotechnology. In *Comprehensive Supramolecular Chemistry II*; Atwood, J. L., Ed.; Elsevier: Oxford, 2017; pp 297−320.

(14) Sharma, A. C.; Jana, T.; Kesavamoorthy, R.; Shi, L.; Virji, M. A.; Finegold, D. N.; Asher, S. A. A General Photonic Crystal Sensing Motif: Creatinine in Bodily Fluids. *J. Am. Chem. Soc.* **2004**, *126*, 2971−2977.

(15) Holtz, J. H.; Asher, S. A. Polymerized Colloidal Crystal Hydrogel Films as Intelligent Chemical Sensing Materials. *Nature* **1997**, *389*, 829−832.

(16) Tanaka, T.; Fillmore, D.; Sun, S.-T.; Nishio, I.; Swislow, G.; Shah, A. Phase Transitions in Ionic Gels. *Phys. Rev. Lett.* **1980**, *45*, 1636−1639.

(17) Flory, P. J. *Principles of Polymer Chemistry*; Cornell University Press, 1953.

(18) Shibayama, M.; Tanaka, T. Volume Phase Transition and Related Phenomena of Polymer Gels. In *Responsive Gels: Volume Transitions I*; Dušek, K., Ed.; Springer: Berlin, Heidelberg, 1993; pp 1−62.

(19) Walker, J.; Kimble, K.; Asher, S. Photonic Crystal Sensor for Organophosphate Nerve Agents Utilizing the Organophosphorus Hydrolase Enzyme. *Anal. Bioanal. Chem.* **2007**, *389*, 2115−2124.

(20) Baler, K.; Michael, R.; Szleifer, I.; Ameer, G. A. Albumin Hydrogels Formed by Electrostatically Triggered Self-Assembly and Their Drug Delivery Capability. *Biomacromolecules* **2014**, *15*, 3625−3633.

(21) Caillard, R.; Remondetto, G. E.; Mateescu, M. A.; Subirade, M. Characterization of Amino Cross-Linked Soy Protein Hydrogels. *J. Food Sci.* **2008**, *73*, C283−C291.

DOI: 10.1021/acsami.9b18191
ACS Appl. Mater. Interfaces 2020, 12, 238−249

(22) Kaehr, B.; Shear, J. B. Multiphoton Fabrication of Chemically Responsive Protein Hydrogels for Microactuation. *Proc. Natl. Acad. Sci. U. S. A.* **2008**, *105*, 8850−8854.
(23) Heck, T.; Faccio, G.; Richter, M.; Thöny-Meyer, L. Enzyme-Catalyzed Protein Crosslinking. *Appl. Microbiol. Biotechnol.* **2013**, *97*, 461−475.
(24) Cai, Z.; Kwak, D. H.; Punihaole, D.; Hong, Z.; Velankar, S. S.; Liu, X.; Asher, S. A. A Photonic Crystal Protein Hydrogel Sensor for Candida Albicans. *Angew. Chem.* **2015**, *127*, 13228−13232.
(25) Cai, Z.; Luck, L. A.; Punihaole, D.; Madura, J. D.; Asher, S. A. Photonic Crystal Protein Hydrogel Sensor Materials Enabled by Conformationally Induced Volume Phase Transition. *Chem. Sci.* **2016**, *7*, 4557−4562.
(26) Zhang, J.-T.; Wang, L.; Luo, J.; Tikhonov, A.; Kornienko, N.; Asher, S. A. 2-D Array Photonic Crystal Sensing Motif. *J. Am. Chem. Soc.* **2011**, *133*, 9152−9155.
(27) Ma, X.; Sun, X.; Hargrove, D.; Chen, J.; Song, D.; Dong, Q.; Lu, X.; Fan, T.-H.; Fu, Y.; Lei, Y. A Biocompatible and Biodegradable Protein Hydrogel with Green and Red Autofluorescence: Preparation, Characterization and In Vivo Biodegradation Tracking and Modeling. *Sci. Rep.* **2016**, *6*, No. 19370.
(28) Fjerbaek, L.; Christensen, K. V.; Norddahl, B. A Review of the Current State of Biodiesel Production Using Enzymatic Transesterification. *Biotechnol. Bioeng.* **2009**, *102*, 1298−1315.
(29) Carrea, G.; Riva, S. Properties and Synthetic Applications of Enzymes in Organic Solvents. *Angew. Chem., Int. Ed.* **2000**, *39*, 2226−2254.
(30) Klibanov, A. M. Improving Enzymes by Using Them in Organic Solvents. *Nature* **2001**, *409*, 241−246.
(31) Jacquet, P.; Daudé, D.; Bzdrenga, J.; Masson, P.; Elias, M.; Chabrière, E. Current and Emerging Strategies for Organophosphate Decontamination: Special Focus on Hyperstable Enzymes. *Environ. Sci. Pollut. Res.* **2016**, *23*, 8200−8218.
(32) Mattos, C.; Ringe, D. Proteins in Organic Solvents. *Curr. Opin. Struct. Biol.* **2001**, *11*, 761−764.
(33) Bhattacharya, R.; Rose, P. W.; Burley, S. K.; Prlić, A. Impact of Genetic Variation on Three-Dimensional Structure and Function of Proteins. *PLoS One* **2017**, *12*, No. e0171355.
(34) Verma, R.; Mitchell-Koch, K. In Silico Studies of Small Molecule Interactions with Enzymes Reveal Aspects of Catalytic Function. *Catalysts* **2017**, *7*, 212−238.
(35) Stepankova, V.; Bidmanova, S.; Koudelakova, T.; Prokop, Z.; Chaloupkova, R.; Damborsky, J. Strategies for Stabilization of Enzymes in Organic Solvents. *ACS Catal.* **2013**, *3*, 2823−2836.
(36) Schmitke, J. L.; Wescott, C. R.; Klibanov, A. M. The Mechanistic Dissection of the Plunge in Enzymatic Activity upon Transition from Water to Anhydrous Solvents. *J. Am. Chem. Soc.* **1996**, *118*, 3360−3365.
(37) Mateo, C.; Palomo, J. M.; Fernandez-Lorente, G.; Guisan, J. M.; Fernandez-Lafuente, R. Improvement of Enzyme Activity, Stability and Selectivity via Immobilization Techniques. *Enzyme Microb. Technol.* **2007**, *40*, 1451−1463.
(38) Cui, J. D.; Jia, S. R. Optimization Protocols and Improved Strategies of Cross-linked Enzyme Aggregates Technology: Current Development and Future Challenges. *Crit. Rev. Biotechnol.* **2015**, *35*, 15−28.
(39) Iyer, P. V.; Ananthanarayan, L. Enzyme Stability and Stabilization—Aqueous and Non-Aqueous Environment. *Process Biochem.* **2008**, *43*, 1019−1032.
(40) Zdarta, J.; Meyer, A.; Jesionowski, T.; Pinelo, M. A General Overview of Support Materials for Enzyme Immobilization: Characteristics, Properties, Practical Utility. *Catalysts* **2018**, *8*, 92−119.
(41) Burton, S. G.; Cowan, D. A.; Woodley, J. M. The Search for the Ideal Biocatalyst. *Nat. Biotechnol.* **2002**, *20*, 37−45.
(42) Sheldon, R. A. Characteristic features and biotechnological applications of cross-linked enzyme aggregates (CLEAs). *Appl. Microbiol. Biotechnol.* **2011**, *92*, 467−477.
(43) Sheldon, R. A.; Schoevaart, R.; Van Langen, L. M. Cross-linked Enzyme Aggregates (CLEAs): A Novel and Versatile Method for Enzyme Immobilization (A Review). *Biocatal. Biotransform.* **2005**, *23*, 141−147.
(44) Fernandez-Lafuente, R. Stabilization of Multimeric Enzymes: Strategies to Prevent Subunit Dissociation. *Enzyme Microb. Technol.* **2009**, *45*, 405−418.
(45) Vitola, G.; Büning, D.; Schumacher, J.; Mazzei, R.; Giorno, L.; Ulbricht, M. Development of a Novel Immobilization Method by Using Microgels to Keep Enzyme in Hydrated Microenvironment in Porous Hydrophobic Membranes. *Macromol. Biosci.* **2017**, *17*, No. 1600381.
(46) Doscher, M. S.; Richards, F. M. The Activity of an Enzyme in the Crystalline State: Ribonuclease S. *J. Biol. Chem.* **1963**, *238*, 2399−2406.
(47) Quiocho, F. A.; Richards, F. M. Intermolecular Crosslinking of a Protein in the Crystalline State: Carboxypeptidase-A. *Proc. Natl. Acad. Sci. U.S.A.* **1964**, *52*, 833−839.
(48) Kartal, F.; Janssen, M. H. A.; Hollmann, F.; Sheldon, R. A.; Kılınc, A. Improved Esterification Activity of Candida Rugosa Lipase in Organic Solvent by Immobilization as Cross-linked Enzyme Aggregates (CLEAs). *J. Mol. Catal. B: Enzym.* **2011**, *71*, 85−89.
(49) Cao, L.; van Langen, L. M.; van Rantwijk, F.; Sheldon, R. A. Cross-linked Aggregates of Penicillin Acylase: Robust Catalysts for the Synthesis of β-Lactam Antibiotics. *J. Mol. Catal. B: Enzym.* **2001**, *11*, 665−670.
(50) Sangeetha, K.; Emilia Abraham, T. Preparation and Characterization of Cross-linked Enzyme Aggregates (CLEA) of Subtilisin for Controlled Release Applications. *Int. J. Biol. Macromol.* **2008**, *43*, 314−319.
(51) Pallares, I. G.; Moore, T. C.; Escalante-Semerena, J. C.; Brunold, T. C. Spectroscopic Studies of the EutT Adenosyltransferase from Salmonella Enterica: Evidence of a Tetrahedrally Coordinated Divalent Transition Metal Cofactor with Cysteine Ligation. *Biochemistry* **2017**, *56*, 364−375.
(52) Lai, K.; Dave, K. I.; Wild, J. R. Bimetallic Binding Motifs in Organophosphorus Hydrolase are Important for Catalysis and Structural Organization. *J. Biol. Chem.* **1994**, *269*, 16579−16584.
(53) Zhang, F.; Cao, L.; Yang, W. Preparation of Monodisperse and Anion-Charged Polystyrene Microspheres Stabilized with Polymerizable Sodium Styrene Sulfonate by Dispersion Polymerization. *Macromol. Chem. Phys.* **2010**, *211*, 744−751.
(54) Zhang, J.-T.; Wang, L.; Lamont, D. N.; Velankar, S. S.; Asher, S. A. Fabrication of Large-Area Two-Dimensional Colloidal Crystals. *Angew. Chem., Int. Ed.* **2012**, *51*, 6117−6120.
(55) Smith, N. L.; Coukouma, A.; Dubnik, S.; Asher, S. A. Debye Ring Diffraction Elucidation of 2D Photonic Crystal Self-Assembly and Ordering at the Air-Water Interface. *Phys. Chem. Chem. Phys.* **2017**, *19*, 31813−31822.
(56) Kanicky, J. R.; Shah, D. O. Effect of Premicellar Aggregation on the pK_a of Fatty Acid Soap Solutions. *Langmuir* **2003**, *19*, 2034−2038.
(57) Mohamad, N. R.; Marzuki, N. H. C.; Buang, N. A.; Huyop, F.; Wahab, R. A. An Overview of Technologies for Immobilization of Enzymes and Surface Analysis Techniques for Immobilized Enzymes. *Biotechnol. Biotechnol. Equip.* **2015**, *29*, 205−220.
(58) Fasano, M.; Curry, S.; Terreno, E.; Galliano, M.; Fanali, G.; Narciso, P.; Notari, S.; Ascenzi, P. The Extraordinary Ligand Binding Properties of Human Serum Albumin. *IUBMB Life* **2005**, *57*, 787−796.
(59) Ghuman, J.; Zunszain, P. A.; Petitpas, I.; Bhattacharya, A. A.; Otagiri, M.; Curry, S. Structural Basis of the Drug-Binding Specificity of Human Serum Albumin. *J. Mol. Biol.* **2005**, *353*, 38−52.
(60) Sułkowska, A. Interaction of Drugs with Bovine and Human Serum Albumin. *J. Mol. Struct.* **2002**, *614*, 227−232.
(61) Evoli, S.; Mobley, D. L.; Guzzi, R.; Rizzuti, B. Multiple Binding Modes of Ibuprofen in Human Serum Albumin Identified by Absolute Binding Free Energy Calculations. *Phys. Chem. Chem. Phys.* **2016**, *18*, 32358−32368.

DOI: 10.1021/acsami.9b18191
ACS Appl. Mater. Interfaces 2020, 12, 238−249

(62) Mew, E. J.; Padmanathan, P.; Konradsen, F.; Eddleston, M.; Chang, S.-S.; Phillips, M. R.; Gunnell, D. The Global Burden of Fatal Self-Poisoning with Pesticides 2006-15: Systematic Review. *J. Affective Disord.* **2017**, *219*, 93−104.
(63) Gotthard, G.; Hiblot, J.; Gonzalez, D.; Elias, M.; Chabriere, E. Structural and Enzymatic Characterization of the Phosphotriesterase OPHC2 from Pseudomonas Pseudoalcaligenes. *PLoS One* **2013**, *8*, No. e77995.
(64) DiCosimo, R.; McAuliffe, J.; Poulose, A. J.; Bohlmann, G. Industrial Use of Immobilized Enzymes. *Chem. Soc. Rev.* **2013**, *42*, 6437−6474.
(65) *The Merck Index: An Encyclopedia of Chemicals, Drugs, and Biologicals*, 11th ed.; Budavari, S., Ed.; Merck: Whitehouse Station, NJ, 2001.
(66) Rastogi, V. K.; Defrank, J. J.; Cheng, T.-c.; Wild, J. R. Enzymatic Hydrolysis of Russian-VX by Organophosphorus Hydrolase. *Biochem. Biophys. Res. Commun.* **1997**, *241*, 294−296.
(67) Tran, D. N.; Balkus, K. J. Perspective of Recent Progress in Immobilization of Enzymes. *ACS Catal.* **2011**, *1*, 956−968.
(68) Wang, P.; Dai, S.; Waezsada, S. D.; Tsao, A. Y.; Davison, B. H. Enzyme Stabilization by Covalent Binding in Nanoporous Sol-Gel Glass for Nonaqueous Biocatalysis. *Biotechnol. Bioeng.* **2001**, *74*, 249−255.
(69) Kreiner, M.; Parker, M. C. Protein-Coated Microcrystals for Use in Organic Solvents: Application to Oxidoreductases. *Biotechnol. Lett.* **2005**, *27*, 1571−1577.
(70) Laothanachareon, T.; Champreda, V.; Sritongkham, P.; Somasundrum, M.; Surareungchai, W. Cross-Linked Enzyme Crystals of Organophosphate Hydrolase for Electrochemical Detection of Organophosphorus Compounds. *World J. Microbiol. Biotechnol.* **2008**, *24*, 3049−3055.

DOI: 10.1021/acsami.9b18191
ACS Appl. Mater. Interfaces 2020, 12, 238−249